Periodic orbits in a simple ray-splitting system

Debabrata Biswas*
Center for Chaos and Turbulence Studies, Niels Bohr Institute, Blegdamsvej 17, Copenhagen Ø, Denmark
(Received 16 April 1996)

We study ray dynamics in a square billiard that allows mode conversion and is parametrized by κ, the ratio of the velocities of the two modes. At $\kappa \to 1^+$, conversion occurs at every reflection and periodic orbits proliferate exponentially. As κ increases beyond $\sqrt{2}$, the collection of daughter rays explore only three momentum directions and mode conversion is progressively inhibited. We provide an algorithm for determining periodic orbits when $\kappa > \sqrt{2}$ and show numerically that exponential proliferation persists around $\kappa \simeq \sqrt{2}$ but as κ increases, a crossover to subexponential behavior occurs for short periods. We discuss these results in the light of conservation laws. [S1063-651X(96)07908-1]

PACS number(s): 05.45.+b, 03.65.Sq

I. INTRODUCTION

Billiards are useful examples of dynamical systems and display the wide variety of phenomena associated with Hamiltonian flows. The ray equations commonly considered follow from a short wavelength expansion of the Schrödinger equation with Dirichlet (or Neumann) boundary conditions. A particle thus moves freely between collisions at the boundary where it suffers specular reflection and one can observe regular or chaotic motion depending on the shape of the boundary. As an example, a square billiard generates regular dynamics that is restricted to a torus in phase space due to the existence of two well behaved constants of motion. In contrast, generic trajectories in the stadium shaped billiard explore the entire constant energy surface and hence the system is ergodic. Moreover, orbits that are nearby initially move exponentially apart with time and hence the system is said to be metrically chaotic.

These differences also show up in the proliferation rates of periodic solutions. In case of regular motion, periodic orbits exist in one-parameter families and their number increases quadratically with time period. In contrast, chaotic dynamics is accompanied by an exponential proliferation of periodic orbits, a phenomenon referred to as topological chaos.

The manner in which periodic orbits organize themselves in closed systems is strongly linked to the existence of sum rules arising from conservation laws. For example, the fact that a particle never escapes implies that for chaotic systems [1,2]

$$\left\langle \sum_p \sum_{r=1}^{\infty} \frac{T_p \delta(t - r T_p)}{|\det(\mathbf{1} - \mathbf{J}_p{}^r)|} \right\rangle = 1, \tag{1}$$

where the summation over p refers to all primitive periodic orbits, T_p is time period, $\mathbf{J}_p$ is the stability matrix evaluated on the orbit and the symbol $\langle . \rangle$ denotes the average value of the expression on the left. Since the periodic orbits are unstable and isolated, $|\det(\mathbf{1} - \mathbf{J}_p{}^r)| \simeq e^{\lambda_p r T_p}$, where λ_p is the Lyapunov exponent of the orbit. The exponential proliferation of orbits is thus implicit in Eq. (1).

For the square billiard though, the appropriate sum rule is [2,3]

$$\left\langle \sum_M \sum_N \frac{1}{(\pi/2)} \frac{4A\delta(t - T_{M,N})}{v^2 T_{M,N}} \right\rangle = 1, \tag{2}$$

where v is the velocity, $T_{M,N}$ is the time period of a periodic orbit with winding numbers (M,N), and A is the area of the billiard. The quadratic law for the number of periodic orbits having time period less than T is thus contained in Eq. (2).

In both cases, the stability of periodic orbits leads to the respective proliferation laws. However, there can exist situations where rays split up at the boundaries of billiards and thus suffer a decay in intensity. The basic conservation law then demands that periodic orbits should proliferate faster than usual to compensate this loss.

Here we explore the case of a square billiard that admits ray splitting and is parametrized by κ, the ratio of velocities of the two modes. For $\kappa \to 1^+$, mode conversion occurs at every reflection from the boundary and daughter rays multiply as 2^k where k denotes the number of reflections. Moreover, the collection of daughter rays (from a single parent) can access an increasing number of momenta directions with time. As κ increases, the range of angle in which conversion can occur at adjacent edges decreases and consequently the average number of daughter rays produced with every reflection decreases. For $\kappa \geq \sqrt{2}$, the possibility of mode conversion is restricted further and daughter rays can access only three momentum directions. Simultaneously, the range of angles at which mode conversion can occur shrinks as κ increases beyond $\kappa_c = \sqrt{2}$. In the limit $\kappa \to \infty$ conversions are not allowed and the system is then a normal billiard without ray splitting.

In the setting described above, we study the proliferation law of periodic paths. In particular, we explore the region $\kappa \geq \sqrt{2}$ and provide an algorithm for determining periodic paths. We find that for $\kappa = 1.429 (> \kappa_c)$, the proliferation law remains exponential but as κ increases further, mode conver-

*On leave from Theoretical Physics Division, Bhabha Atomic Research Centre, Bombay 400 085, India. Electronic address: biswas@kaos.nbi.dk

sion is inhibited and the proliferation law shows a crossover to subexponential behavior for short periods.

Before discussing these in detail, it is important to note that periodic orbits form the skeleton on which modern semiclassics is built [4] and are used to understand the spectrum in quantum systems. In elastodynamics where mode conversion does occur, studies of the statistical properties of the resonance spectrum are influenced to a large extent by these considerations [5,6]. In fact, a Fourier transform of the resonance spectrum provides evidence of the role of periodic orbits in elastodynamics [5]. The present study is thus significant in that it provides the first systematic computation of periodic orbits and underscores its complex organization even in simple geometries.

In the following section, we describe in more detail the system that we study and analyze the dynamics of the converted rays. Section III deals with the algorithm for determining periodic orbits and our numerical results are discussed in Sec. IV.

II. A SIMPLE RAY-SPLITTING SYSTEM

Ray splitting is a common phenomenon in geometrical optics and can be observed in several other situations [7–9]. The propagation of elastomechanical waves in solids is an example that is of much current interest [5,6] and we study here the short wavelength limit of this problem for the isotropic case in two dimensions. For small displacements, the wave motion is governed by the Navier equation [10]

$$\mu\nabla^2\mathbf{u}+(\lambda+\mu)\nabla\nabla\cdot\mathbf{u}=\rho\partial^2\mathbf{u}/\partial t^2, \tag{3}$$

where $\mathbf{u}$ is the displacement, λ and μ are the two Lamé constants [11], and ρ is the density. It is common to express the displacement as a sum of two parts generated, respectively, by a scalar and a vector potential ($\mathbf{u}=\mathbf{u}_1+\mathbf{u}_2$ where $\mathbf{u}_1=\nabla\phi$ and $\mathbf{u}_2=\nabla\times\mathbf{B}$) so that Eq. (3) separates into two second-order equations [10]

$$\nabla^2\phi=\frac{1}{c_P^2}\partial^2\phi/\partial t^2, \tag{4}$$

$$\nabla^2\mathbf{B}=\frac{1}{c_S^2}\partial^2\mathbf{B}/\partial t^2, \tag{5}$$

where $c_P^2=(\lambda+2\mu)/\rho$ and $c_S^2=\mu/\rho$. The medium thus has two natural velocities, c_P and c_S where the subscripts P and S refer to the pressure (longitudinal) and shear (transverse) waves, respectively. The two waves interact only at the boundaries where they may suffer mode conversion.

Consider, for example, an S or a P wave incident on a planar stress-free (tractionless) boundary. The reflected part consists in general of both an S and a P wave and the reflection law involving an S and a P wave is given by Snell's relation [10]

$$\cos(\theta_P)=\kappa\cos(\theta_S), \tag{6}$$

where the angles are measured with respect to the tangent at the collision point on the boundary and $\kappa=c_P/c_S$. When the reflected and incident wave belong to the same type (both S or both P), the angle of reflection equals the angle of incidence. Note that Eq.(6) implies the existence of a critical angle $\theta_C=\cos^{-1}(1/\kappa)$. For $\theta_S<\theta_C$, no conversion can occur and the wave suffers only a specular reflection.

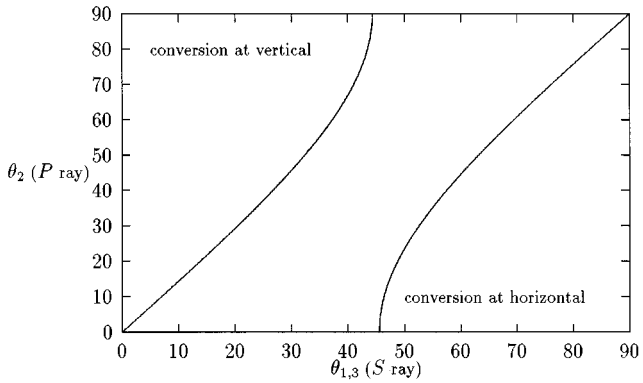

FIG. 1. The map shows the relationship between the angles of the S and P ray on conversion at $\kappa=1.429$. All angles are measured with respect to the X axis; i.e., horizontal edge. Notational details can be found in the text.

The incident and reflected amplitudes are also determined by the boundary conditions. For $S\rightarrow S+P$ process, and for the case where the S wave polarization lies in the plane of incidence, the intensities carried away by the reflected S and P wave are [10]

$$I_{SS}=\left|\frac{\sin(2\theta_S)\sin(2\theta_P)-\kappa^2\cos^2(2\theta_S)}{\sin(2\theta_S)\sin(2\theta_P)+\kappa^2\cos^2(2\theta_S)}\right|^2 \tag{7}$$

and $I_{SP}=1-I_{SS}$, respectively. Similarly, for the $P\rightarrow S+P$ process, $I_{PP}=I_{SS}$ and $I_{SP}=I_{PS}$ provided again that the S wave polarization lies in the plane of incidence. In general, the full three-dimensional problem requires a decomposition of the polarization vector into components normal and parallel to the plane of incidence. The component in the plane undergoes the process described above while the normal component suffers no conversion.

The small-wavelength limit of this wave motion restricted to a plane can be treated as the relevant ray-tracing problem in two-dimensions. The geometry we consider here is a square billiard of length $L=\pi/2$. In a situation where no mode conversion occurs, the square billiard is integrable and its periodic orbits increase quadratically with length. The corresponding Schrödinger equation can be solved easily and the quantum spectrum is described exactly by periodic orbits. The situation in elasdodynamics is, however, quite the opposite and the only resonances known analytically form a small fraction of the total number [10]. To the best of our knowledge, the ray-tracing problem in this geometry has not been studied before and we proceed to understand that now.

The parameter range that is physically accessible is $\kappa>1$ and as an example we study the case $\kappa=1.429$. Figure 1 illustrates the conversions that can occur in this system. For the sake of visualization, it is convenient to consider an unfolded trajectory in the full plane generated by reflections of the fundamental domain about its sides (see Fig. 2). A reflected trajectory without conversion thus continues through the boundary without any change in angle while a ray that has suffered conversion is equivalent to a refracted

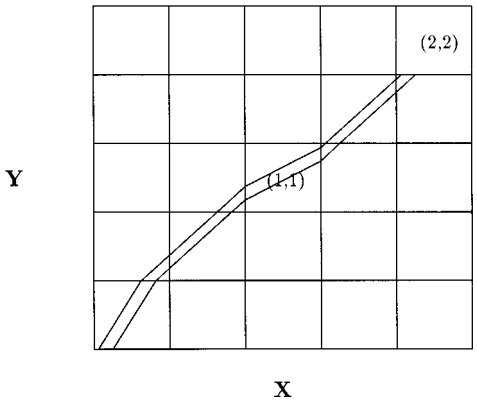

FIG. 2. Two unfolded periodic orbits belonging to the same family with winding number (2,2) and symbol itinerary (S',P,S,P'). Note the small segments of P ray between S' and P as well as S and P'.

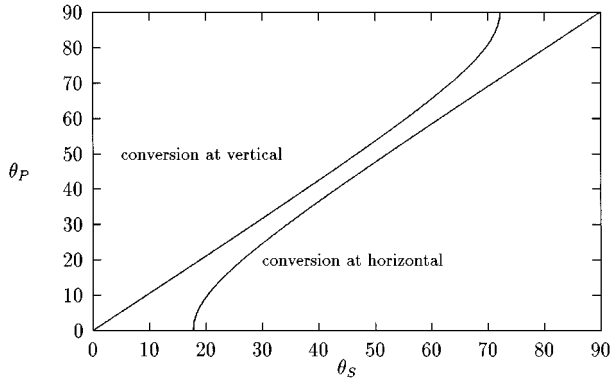

FIG. 3. The map shows the conversions possible at $\kappa=1.05$. The angles θ_S and θ_P denote, respectively, the angles of the S and P ray measured with respect to the X axis (horizontal edge). Note that there is a range of angles where conversion can occur at both the horizontal and vertical edges. This is referred to as an *overlap*.

ray that undergoes a change in angle. A cell identical to the fundamental domain can then be labeled by the winding numbers (M,N) where $2ML$ is the displacement of any point in the cell along the X axis and $2NL$ along the Y axis. Figure 2 shows the cells with winding numbers (1,1) and (2,2).

Consider then a family of S rays at an angle θ_1 with respect to the horizontal edge (X axis, see Fig. 2). For $\theta_1<\pi/2-\theta_C$, conversion to a P ray can occur only at the vertical edge (Y axis, see Fig. 2). The P ray at an angle θ_2 (measured from the X axis), can, however, reconvert to an S ray at both the vertical and the horizontal edges. If it reconverts at the vertical edge, the resultant reflected S ray is again at an angle θ_1 while if reconversion occurs at the horizontal edge, the S ray (which we denote by S') is at an angle $\theta_3>\theta_1$ (see Fig. 1). The first possibility requires no further analysis while for the S ray at an angle θ_3, reconversion can occur only at the horizontal edge and hence generates a P ray at angle θ_2. An identical process occurs if $\theta_1>\theta_C$ except that edges are now interchanged. For $\pi/2-\theta_C<\theta_1<\theta_c$ (see Fig. 1) and for $\theta_1=0$ or $\pi/2$, there is no conversion and the orbit continues with the same intensity. This exhausts all possibilities so that there are only three directions $\{\theta_1,\theta_2,\theta_3\}$ that all rays originating from a given parent ray can explore.

As κ increases, the two branches in the map of Fig. 1 move apart and the range of angles at which conversion can occur at either the vertical or horizontal edge shrinks. However, the scenario described above continues to hold whenever conversion does occur and the daughter rays produced explore only three momenta directions.

As κ decreases however, the branches in the map (of Fig. 1) come closer and meet at $\kappa_c=\sqrt{2}$. As κ decreases below κ_c, there is a range of angles in which conversion occurs both at the horizontal and vertical edge as shown in Fig. 3. Consequently, the number of directions accessible to all daughter rays from a single parent increases as well. As κ decreases further, the overlap increases and at $\kappa\rightarrow 1^+$, conversion can occur at both the horizontal and vertical edge for any initial angle. Thus rays split with every reflection and the number of daughter rays grows as 2^k where k denotes the number of reflections. The collection of all daughter rays now explore an increasing number of momentum directions in sharp contrast to the case when $\kappa>\kappa_c$.

Note that in all cases, the orbits are marginally unstable as in the case when no conversion occurs. This can be verified by linearizing the neighborhood and looking at the eigenvalues of the Jacobian matrix. Periodic rays thus occur in families and their extent is limited by the vertices where adjacent parallel rays meet a horizontal and a vertical edge, respectively, and convert differently.

III. PERIODIC ORBITS

We now turn to a study of periodic orbits in such a system and provide an algorithm for determining them when $\kappa>\kappa_c$. We first note that unlike a normal square billiard, each set of winding numbers (M,N) can correspond to more than one periodic solution. The total length, l_S, of all S segments (at angle θ_1) in a periodic trajectory is such that $l_S\cos(\theta_1)=m_1L$, where m_1 is an integer and L is the size of the square. Similarly, the total length, $l_{S'}$ of S' segments in a periodic trajectory is such that $l_{S'}\sin(\theta_3)=n_1L$ where n_1 is again an integer. It follows then that the total length, l_P of all P segments in a trajectory with winding numbers (M,N) is such that

$$l_P\cos(\theta_2)=[(2M-m_1)L-n_1L\cot(\theta_3)]. \tag{8}$$

On equating the total projected length of the trajectory along the vertical edge $[l_S\sin(\theta_1)+l_P\sin(\theta_2)+l_{S'}\sin(\theta_3)]$ to $2NL$ we obtain

$$m_1\tan(\theta_1)+[(2M-m_1)-n_1\cot(\theta_3)]\tan(\theta_2)=(2N-n_1), \tag{9}$$

where m_1 can vary from 0 to $2M$ while n_1 can vary from 0 to $2N$. Note that θ_2 and θ_3 can be expressed in terms of θ_1 so that for a given value of (m_1,n_1), the root of Eq. (9) (if any) can be determined. However not all (m_1,n_1) admit real solution though in general any set of winding numbers, (M,N) allows more than one periodic orbit. The case $m_1=2M,n_1=0$ corresponds to a normal periodic orbit that suffers no conversion.

The total length of all S ray segments in any trajectory with winding numbers (M,N) and labeled by (m_1,n_1) is $l_S+l_{S'}=Lm_1/\cos(\theta_1)+Ln_1/\sin(\theta_3)$ while the length of P ray segments put together is $l_P=[2M-m_1-n_1\cot(\theta_3)]L/\cos(\theta_2)$. The time period of the trajectory is thus $(l_S+l_{S'})/c_S+l_P/c_P$.

Clearly, these S, S' and P segments can be arranged in several ways so that an orbit with a given (M,N,m_1,n_1) will in general be degenerate. In order to compute the degeneracy, it is necessary to construct symbol itineraries that are not related by cyclic permutation. It turns out that four distinct symbols, S,S',P,P' together with the winding numbers (M,N) specify a trajectory. Here $S(P)$ and $S'(P')$ refer to a single stretch of $S(P)$ ray between two consecutive vertical and horizontal edges, respectively, (see Fig. 2) though it must be noted that P and P' have the same angle θ_2 where as S and S' are at angles θ_1 and θ_3, respectively. Also, the total length of all P segments is in general not equal to $m_2L/\cos(\theta_2)+n_2L/\sin(\theta_2)$ where m_2 and n_2 are integers that count the number of P and P' segments, respectively. This is due to the fact that there exist small segments of P ray joining adjacent vertical and horizontal edges.

Consider for example the case with $(m_1,n_1,m_2,n_2)=(1,1,1,1)$ [12]. There are six distinct itineraries: (S,S',P,P'), (S,S',P',P), (S,P,S',P'), (S,P,P',S'), (S,P',S',P), (S,P',P,S'), and some of these correspond to periodic trajectories with winding numbers, $(M,N)=(2,2)$ [13]. It is implicit, however, that small segments of P rays joining adjacent vertical and horizontal edges exist, whenever the following two symbols occur consecutively in an itinerary: (S,S'),(S',P),(S,P') or (P,P'). Figure 2 illustrates this for (S',P,S,P') with $(M,N)=(2,2)$.

Finally it is important to remark that the above symbols do not specify a trajectory uniquely and it is possible that more than one itinerary corresponds to the same orbit. This occurs when the total length of a single P segment in a trajectory is such that it hits at least two vertical and also two horizontal edges.

For $\kappa<\kappa_c$, the analysis gets increasingly complicated though as $\kappa\to1^+$, all daughter rays born out of a parent periodic orbit at an angle $\theta_1=\tan^{-1}(N/M)$ are eventually periodic with the same length (for $c_S=c_P=1$, the time period equals the length). The degeneracy is thus $2^{2(M+N)}$ so that the density of orbit lengths can be expressed as

$$d(l)=\sum_M\sum_N \delta(l-2L\sqrt{M^2+N^2})e^{2(M+N)\ln2}. \quad (10)$$

The average proliferation rate can thus be obtained by integrating over M and N as

$$d_{av}(l)=\int dM\int dN\,\delta(l-2L\sqrt{M^2+N^2})e^{2(M+N)\ln2} \quad (11)$$

$$=\int_0^{\pi/2}d\theta\int dr\,\frac{r}{4L^2}\delta(l-r)e^{r\sqrt{2}\ln2\cos(\theta-\pi/4)/L}, \quad (12)$$

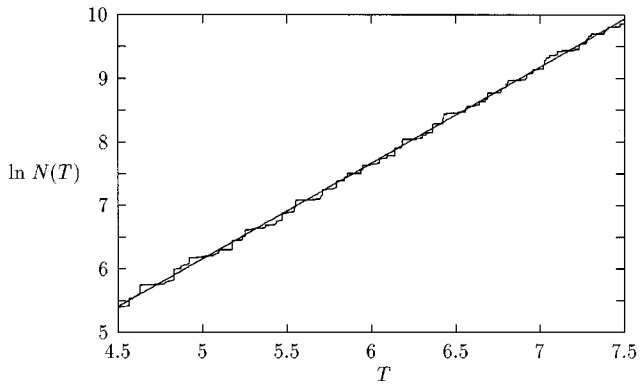

FIG. 4. A plot of $\ln N(T)$ as a function of T together with the best fitting straight line. Here $N(T)$ counts the number of periodic orbits that suffer conversion and have periods less than or equal to T. The growth exponent as derived from the slope is 1.509.

where $2LM=r\cos(\theta)$ and $2LN=r\sin(\theta)$. The r integration is trivial and the θ integration can be evaluated asymptotically for large l using the Laplace method [14]. We finally obtain

$$d_{av}(l)=\frac{l}{4L^2}\left(\frac{\pi}{2hl}\right)^{1/2}e^{hl}, \quad (13)$$

where the growth exponent $h=(\sqrt{2}/L)\ln2$. For $L=\pi/4$, $h=1.248$.

As $\kappa\to\infty$, no conversion is allowed and the average density of periodic orbits is then

$$d_{av}(l)=\frac{2\pi l}{16L^2}. \quad (14)$$

With this background, we now present some numerical results on the proliferation rate of periodic orbits for $\kappa>\kappa_c$.

IV. NUMERICAL RESULTS

We first consider the case, $\kappa=1.429$ and choose $c_S=1$ and $c_P=\kappa$. Using the procedure outlined above, we have generated all periodic orbits that have time periods less than 7.5. We then construct the staircase function $N(T)=\Sigma_i\Theta(T-T_i)$ which counts the number of periodic orbits with $T_i\leq T$. Figure 4 shows a plot of $\ln N(T)$ as a function of T together with the best fitting straight line. The fit is good indicating an exponential proliferation of periodic orbits. The slope, which is a measure of the growth rate, equals 1.509.

Note that a direct comparison with the growth rate at $\kappa\to1^+$ (obtained in Sec. III) is not possible due to the fact that the velocities at $\kappa=1.429$ are necessarily different. Assuming that all conversions are allowed, the mean velocity required to achieve a growth rate of 1.5 is about 1.2.

We next consider the cases when κ equals 8 and 30 and choose $c_S=1/\kappa$ and $c_P=1$. The range of angles which permit conversion at $\kappa=8$ is now much smaller and a large fraction of periodic orbits do not undergo any conversion for the time periods considered. The proliferation rate is thus subexponential (for a plot, see Fig. 5).

For $\kappa=30$, conversion is further inhibited as the range of

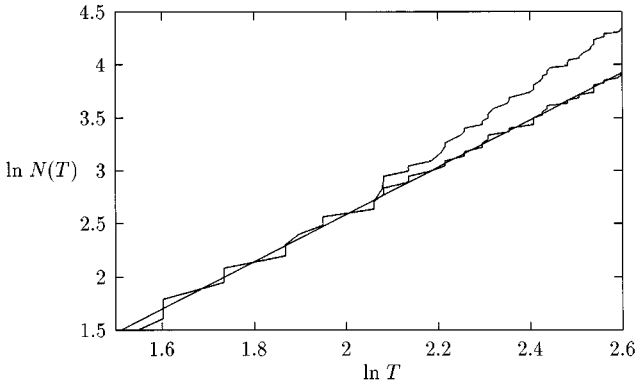

FIG. 5. The proliferation law for $\kappa=8$ (upper curve) and $\kappa=30$ (lower curve). Note that we plot $\ln N(T)$ as a function of $\ln T$. Also shown is the best fitting straight line for $\kappa=30$.

angles (in which conversion is allowed) becomes smaller still. This is evident in Fig. 5 where we plot $\ln N(T)$ as a function of $\ln T$ for $\kappa=8$ and 30. The curve for $\kappa=30$ has a good linear fit with slope 2.22 indicating a power law behavior (note that the exponent is expected to be 2 in the limit $\kappa\rightarrow\infty$). The curve for $\kappa=8$ follows this until $\ln T\simeq 2$ and then increases as more converted orbits are included.

This substantiates our analysis and shows that with a decrease in the average number of conversions as κ increases, the proliferation law for short periods shows a crossover from exponential to power law behavior. However for large but finite κ, exponential proliferation is eventually expected to dominate for large T though these orbits are not easily accessible to computations.

V. DISCUSSIONS AND CONCLUSIONS

We have, in the preceding sections, analyzed a simple ray-splitting system and shown that as the parameter κ increases from 1^+, mode conversion is progressively inhibited and does not take place with every reflection at the boundary. This shows up in the proliferation law of periodic orbits as well. Surprisingly, exponential proliferation persists for $\kappa\simeq\sqrt{2}$ where the number of directions accessible to the daughter rays is only three. For short periods, there is a crossover to subexponential proliferation with increasing κ since conversion can occur in a progressively shrinking range of angles that are (nearly) parallel to the two edges and converted periodic orbits are thus longer on an average.

In terms of conservation laws, the decay in intensity that accompanies splitting must be compensated by a faster proliferation of periodic orbits, though not necessarily of the exponential kind. The sum rule for ray splitting, however, needs to be derived in order to be more specific, though heuristically, its form should be similar to Eq. (2) with each term having an additional factor representing the intensity loss. This is an important area to explore for sum rules can be put to practical use, for example, in checking whether all periodic orbits up to a certain length have been determined.

Our computations were limited by the fact that a set of four symbols together with the winding numbers were necessary to label periodic orbits. We have, in each case included all periodic orbits with symbols strings of length 10 and the period T up to which all periodic orbits are available is decided by the shortest orbit with symbol string of length greater than 10. For boundary shapes leading to hyperbolicity, the complexities increase making longer orbits practically inaccessible to computations. Thus, even though our results for larger values of κ are limited to short orbits, they are significant in this light.

ACKNOWLEDGMENTS

The author acknowledges valuable help from Mark Oxborrow and Per Rosenqvist and several useful discussions with Bertrand Georgeot, Predrag Cvitanović, Gregor Tanner, and Niall Whelan.

[1] P. Cvitanović and B. Eckhardt, J. Phys. A **24**, L237 (1991).
[2] J. H. Hannay and A. M. Ozorio de Almeida, J. Phys. A **17**, 3429 (1984).
[3] D. Biswas (unpublished).
[4] M. C. Gutzwiller, *Chaos in Classical and Quantum Mechanics* (Springer, New York, 1990).
[5] D. Delande, D. Sornette, and R. Weaver, J. Acous. Soc. Am. **96**, 1873 (1994).
[6] C. Ellegaard, T. Guhr, K. Lindemann, H. Q. Lorensen, J. Nygård, and M. Oxborrow, Phys. Rev. Lett. **57**, 1546 (1995).
[7] L. Couchman, E. Ott, and T. M. Antonsen, Jr., Phys. Rev. A **46**, 6193 (1992).
[8] R. Bluemel, T. Antonsen, Jr., B. Georgeot, E. Ott, and R. E. Prange, Phys. Rev. Lett. **76**, 2476 (1996); Phys. Rev. E **53**, 3284 (1996).
[9] R. E. Prange, E. Ott, T. Antonsen, Jr., B. Georgeot, and R. Bluemel, Phys. Rev. E **53**, 207 (1996).
[10] K. F. Graf, *Wave Motion in Elastic Solids* (Dover, New York, 1991).
[11] Other elastic constants such as Young's modulus, Poisson's ratio, and the bulk modulus can be expressed in terms of the Lamé constants.
[12] m_2 and n_2 can vary between 0 and $[l_P\cos(\theta_2)/L]$ or $[l_P\sin(\theta_2)/L]$, respectively.
[13] In general two trajectories with different (M,N) can have the same (m_1,n_1,m_2,n_2).
[14] A. Erdelyi, *Asymptotic Expansions* (Dover, New York, 1956).